

Anomaly Unveiled: Securing Image Classification against Adversarial Patch Attacks

Nandish Chattopadhyay, Amira Guesmi, and Muhammad Shafique
eBrain Lab, Division of Engineering, New York University (NYU) Abu Dhabi, UAE

Abstract—Adversarial patch attacks pose a significant threat to the practical deployment of deep learning systems. However, existing research primarily focuses on image pre-processing defenses, which often result in reduced classification accuracy for clean images and fail to effectively counter physically feasible attacks. In this paper, we investigate the behavior of adversarial patches as anomalies within the distribution of image information and leverage this insight to develop a robust defense strategy. Our proposed defense mechanism utilizes a clustering-based technique called DBSCAN to isolate anomalous image segments, which is carried out by a three-stage pipeline consisting of Segmenting, Isolating, and Blocking phases to identify and mitigate adversarial noise. Upon identifying adversarial components, we neutralize them by replacing them with the mean pixel value, surpassing alternative replacement options. Our model-agnostic defense mechanism is evaluated across multiple models and datasets, demonstrating its effectiveness in countering various adversarial patch attacks in image classification tasks. Our proposed approach significantly improves accuracy, increasing from 38.8% without the defense to 67.1% with the defense against LaVAN and GoogleAp attacks, surpassing prominent state-of-the-art methods such as LGS [1] (53.86%) and Jujutsu [2] (60%).

I. INTRODUCTION

Adversarial manipulations pose a significant challenge to the resilience and effectiveness of well-trained deep neural network (DNN) architectures [3]–[8]. In such scenarios, adversaries strategically introduce perturbations to test samples, leading to noticeable disruptions in the model’s ability to accurately predict outcomes. A notable form of these attacks involves the insertion of localized patches into test images, exploiting vulnerabilities and causing the DNN model to err in crucial tasks such as image classification or object detection [9]–[11].

Patch-based attacks are recognized as a practical form of adversarial manipulation, valued for their adaptability, especially in scenarios with limited accessibility [3], [12], [13]. Unlike traditional adversarial methods that require extensive perturbations spanning the entire target object, patch-based attacks exhibit a localized nature. These attacks function like discrete stickers, making them easy to apply to potential targets, reflecting real-world situations where adversaries may face resource or access constraints. The subtle attributes of patch-based attacks contribute to their elusive nature, emphasizing the urgent need for the rapid deployment of robust defense mechanisms.

However, these defenses are prone to generating false positives [1] and face challenges in accurately distinguishing

between adversarial and clean samples. Additionally, in certain instances, these defenses may inadvertently remove or alter crucial features [14], [15], resulting in the degradation of the model’s performance even on benign samples.

Adversarial patches exhibit characteristics of outliers or anomalies within the distribution of input images. The adversarial noise embedded within these patches diverges significantly from the signal or information present in the rest of the sample. Leveraging advanced anomaly detection techniques facilitates the identification and segregation of these patches in instances where they deviate from the broader image distribution. This is particularly useful in developing practical adversarial defenses against such patch based attacks.

A. Contribution

The primary contributions of this paper is mentioned here:

- We introduce a novel defense mechanism against adversarial patch attacks. Our approach involves isolating the region in the image containing the patch as an anomaly and subsequently blocking the adversarial information.
- We demonstrate the distinctive informational disparities inherent in adversarial patches, offering invaluable insights crucial for the development of resilient defense strategies against adversarial patch attacks.
- We propose a three-step pipeline for implementing our defense mechanism, comprising a Segmenting phase, an Isolating phase, and a Blocking phase. Initially, the Segmenting phase divides the image into parts, which are then subjected to a clustering algorithm (DBSCAN) [16], [17] to identify segments containing adversarial noise. Subsequently, we replace these identified segments with the mean pixel value to neutralize the adversarial patch.
- Our defense mechanism is model-agnostic and demonstrates impressive performance, achieving up to 85% recovery on adversarial samples in image classification tasks across various datasets, adversarial patches, and neural architectures.

II. THEORETICAL BACKGROUND

A. Adversarial Patches

Adversarial patches constitute a distinct subset of adversarial perturbations targeting localized areas within images to deceive classification models. These attacks exploit the susceptibility of models to localized changes, aiming to introduce subtle modifications that significantly affect the model’s

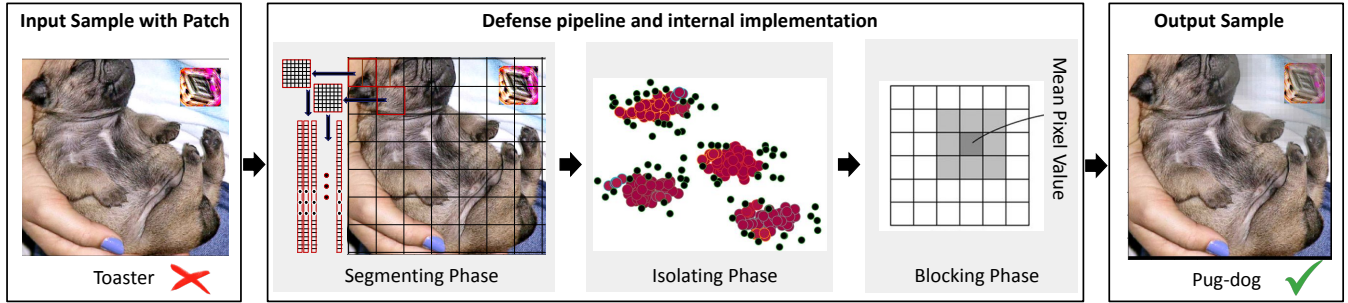


Fig. 1: Detailed diagram of our proposed methodology.

predictions. By exploiting the model’s reliance on specific features or patterns, adversaries create patches intended to mislead the model into either misclassifying the image or interpreting it differently from its true representation.

1) *LaVAN* [18]: *LaVAN* is a method designed to create localized and discernible patches that are applicable to a variety of images and positions. This technique entails iteratively training the patch by selecting a random image and positioning it at a randomly selected location. This iterative training ensures that the model can learn the distinctive characteristics of the patch across diverse scenarios, thereby improving its transferability and overall efficacy.

2) *GoogelAp* [19]: The *GoogelAp* technique offers a pragmatic method for real-world attacks, contrasting with L_p -norm-based adversarial perturbations, which require object capture using a camera. *GoogelAp* generates universal patches adaptable to diverse locations. Additionally, the attack incorporates Expectation over Transformation (EOT) [20] to enhance the effectiveness of the generated adversarial patch.

B. Attack Formulation

In the context of image classification, let’s consider a deep learning-based image classifier denoted as $f : X \rightarrow Y$. Here, X represents the set of images, and Y represents the set of labels. The classifier maps an input image x from X to an output class with label y from Y . An adversarial example, represented as x^* , is defined as:

$$x^* \in X, \quad f(x) = y, \quad f(x^*) = y^*, \quad y \neq y^*$$

Here, y^* represents the targeted label, and x^* is the adversarial example generated from the original input x . Specifically in the context of patch-based attacks, a segment of the image is substituted with the patch, symbolized as P .

Technically, the formulation of an adversarial example with a generated patch is expressed as:

$$x^* = (1 - m_P) \odot x + m_P \odot P$$

Here, \odot denotes component-wise multiplication, where P represents the adversarial patch, and m_P is a mask matrix that governs the shape, size, and pasting position of the patch. Specifically, the pasting area is assigned a value of 1, while the remaining areas are set to 0. To ensure the patch P remains

input-agnostic, it undergoes training across a range of images. *LaVAN* [18] adopts a fixed location strategy, where the patch is trained to stay at a predetermined position for each input $x \in X$. Conversely, *GoogelAp* employs a random location approach, training the patch to be applied at any position within the image. Furthermore, to enhance the robustness and physical realizability of patch P , *GoogelAp* utilizes an Expectation over Transformation (EOT) framework [20]. EOT encompasses various environmental transformations T , such as translation, rotation, or changes in lighting conditions, applied to x . Adversarial examples generated under these diverse transformations aim to maintain their efficacy, thereby enhancing the attack’s overall effectiveness.

C. Adversarial patches as anomalies

To study whether the adversarial noise contained in the adversarial patches belong to a different distribution or not, as compared to the clean images, we make use of a distance metric to measure the distance between the overall distribution of the image and the adversarial patch. Specifically, we split the adversarial image along with the patch into segments (as described in Section III) and fit a distribution to it, and calculate the Mahalanobis distance of every segment from that distribution [21]. The Mahalanobis distance [22] is a distance metric which is designed to measure the distances of data points with respect to a distribution. Formally, for a probability distribution Q on \mathbb{R} , which has the mean $\mu = (\mu_1, \dots, \mu_N)^T$, a positive definite covariance matrix S , then for any point $x = (x_1, \dots, x_N)^T$ for the said distribution Q , the Mahalanobis distance is [23]:

$$d_M(x, Q) = \sqrt{(x - \mu)^T S^{-1} (x - \mu)}$$

For our case, the x_i s are the segments created as part of the Segmentation phase. Once we calculate the Mahalanobis distance for every such segment, and plot them, we observe a bi-modal distribution in Figure 2, with the distance measured for the segments lying on the adversarial patch having a significantly higher value of Mahalanobis distance than the rest. This is a clear indication that the patch contains informational variability that is different from the rest of the image and can be isolated as anomalies.

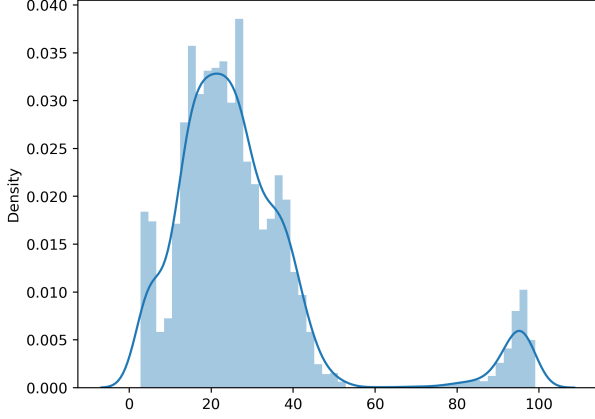


Fig. 2: Plot of Mahalanobis distances of segments to represent anomalous behaviour of adversarial patches as seen in the bi-model distribution.

D. Anomaly Detection with DBSCAN

We make use of the insight that adversarial patches contain anomalous features when compared to clean image samples to propose a defense mechanism. This is achieved using an unsupervised clustering technique called DBSCAN [16]. This is a density based algorithm for discovering clusters in large spatial datasets with noise. The DBSCAN algorithm [17] takes a dataset, denoted as $data$, a distance function $distFunc$ and two hyper-parameters eps and $minPts$ as inputs. The eps -neighbourhood of any data sample p is denoted by $N_{eps}(p)$, and is given by the following condition: $N_{eps}(p) = \{q \in data \mid distFunc(p, q) \leq eps\}$. Also, this data point p in consideration is *directly density reachable* as per definition if both the conditions $p \in N_{eps}(q)$ and $|N_{eps}(q)| \geq minPts$ are simultaneously satisfied. Any data point p is *density reachable* if there are points p_1, \dots, p_n , $p_1 \approx q$, $p_n = p$, such that p_{i+1} is *directly density reachable* from p_i . Similarly, the data point p is *density connected* to a point q , if there exists a point o such that both p and q are *density reachable* from o , for the set eps and $minPts$ value. These definitions help us in formalizing the building of the clusters using the DBSCAN algorithm. A cluster C (where $C \subseteq data$) is formed from the $data$ if the following conditions are satisfied: $\forall p, q$, if $p \in C$ and q is *density reachable* from p for the corresponding eps and $minPts$, then $q \in C$; and $\forall p, q \in C$, p is *density connected* to q for the corresponding eps and $minPts$. These two conditions are called the Maximality and Connectivity conditions. If we consider the k clusters so generated to be C_1, \dots, C_k , then the anomalies are the data points that have the label *Noise*, where those points do not belong to any cluster C_i , such that $Noise = \{p \in data \mid \forall i \text{ where } p \notin C_i\}$ for a set eps and $minPts$ value [24], [25]. The details of the algorithm is mentioned in Algo 1.

Algorithm 1: DBSCAN($data, distFunc, eps, minPts$)

```

 $C \leftarrow 0$ 
for ( $P \in data$ ):
  if ( $label(P) \neq undefined$ ):
     $N \leftarrow Search(data, distFunc, P, eps)$ 
  end if
  if ( $|N| < minPts$ ):
    label( $P$ )  $\leftarrow$  Noise
  end if
   $C \leftarrow C + 1$ 
  label( $P$ )  $\leftarrow$   $C$ 
  Set  $S \leftarrow N \setminus \{P\}$ 
  for ( $Q \in S$ ):
    if ( $label(Q) == Noise$ ):
      label( $Q$ )  $\leftarrow$   $C$ 
    end if
    if ( $label(Q) == undefined$ ):
      label( $Q$ )  $\leftarrow$   $C$ 
       $N \leftarrow Search(data, distFunc, Q, eps)$ 
      if ( $|N| \geq minPts$ ):
         $S \leftarrow S \cup N$ 
      end if
    end if
  end for
end for
Initialize  $Y = (y_1, \dots, y_n)$ 
for ( $i \in (1, \dots, n)$ ):
   $y_i \leftarrow label(P)$ 
end for
return  $Y$ 

```

Algorithm 2: Search($data, distFunc, Q, eps$)

```

 $N \leftarrow Q$ 
for ( $P \in data$ ):
  if ( $distFunc(Q, P) \leq eps$ ):
     $N \leftarrow N \cup \{P\}$ 
  end if
end for
return  $N$ 

```

III. DEFENSE TECHNIQUE

As illustrated in Figure 1, our proposed defense mechanism has a three stage pipeline, that we have created to isolate the area of the image containing the adversarial patch and thereby, mitigating it. The first part of the process is the Segmenting Phase, which chops up the image into kernels using a moving window, which parses the entire image. Thereafter, in the Isolating Phase, the generated segments are used as inputs to the clustering mechanism. The segments identified as the anomalies are subjected to the Blocking Phase, where the adversarial noise is destroyed. The complete algorithm is described in details in Algo 3.

A. Segmenting Phase

We parse the image using a moving window of a fixed kernel size and a specific stride length, and chop us the image into segments which have partial overlap. Since the kernel size and the stride length are both hyper-parameters to the system, the amount of overlap can be varied. These segments are converted to long vectors, which is used as the data samples for the clustering algorithm subsequently.

B. Isolating Phase

The segments, generated through the earlier step, serve as the data samples on which the anomaly detection method is applied. It may be noted here that the goal is to identify those segments which correspond to the part of the image that contains the adversarial patch. We propose to use clustering for this purpose, specifically DBSCAN [16], which is very efficient in identifying noise or anomalous samples, which do not belong to any of the clusters. Notably, for the most optimal performance, we tune the parameters of the DBSCAN algorithm, which are eps and the minimum number of points in a cluster $minPts$. The details and the significance of these hyper-parameters and how they help in the DBSCAN clustering is explained in details in Section II. Once we run the DBSCAN algorithm, the labels corresponding to all the samples are noted (labels signify the associated cluster ID for each sample/segment) and the samples which have been labelled as *Noise* are identified as the anomalies.

C. Blocking Phase

Once some of the segments are identified as the those with anomalous behaviour with respect to the other set of segments corresponding to the rest of the image, we use the *Replace()* function to set all pixels within the segment to a common value. We experimented with the minimum, mean and maximum values of the segment and our observations provide evidence of superior performance of the mean pixel values. Therefore, in all our experiments, we have used the average value of the pixels (channel-wise for the colours).

IV. EVALUATION

In this section, we conduct a comprehensive evaluation of the efficacy of our proposed defense mechanism.

A. Experimental Setup

1) *Datasets and Networks*: We conducted our defense evaluation on the ImageNet dataset [26], employing three pretrained deep neural networks (DNNs) accessible in the TorchVision library: ResNet-50 [27], ResNet-152 [27], and VGG-19 [28]. These widely recognized models were selected to facilitate a thorough assessment across various DNN architectures and model complexities.

Algorithm 3: Anomaly Detection and Mitigation

IN : S : sample image, k : size of kernel, $strlen$: length of stride, eps : DBSCAN parameter, $minPts$: minimum size of clusters
OUT : S' : Image with neutralised patch
*/*Segmenting_Phase*/*
 Create n segments $X \leftarrow (x_1, \dots, x_n)$ from sample S , using $= k$ as kernel size and $strlen$ as stride length
*/*Isolating_Phase*/*
 $Y = DBSCAN(X, eps, minPts)$ (Algo 1)
initialize $A = \{\}$
for ($i \in (1, \dots, n)$):
 if ($y_i == Noise$):
 $A \leftarrow x_i$
 end if
end for
*/*Blocking_Phase*/*
 Set $r = Size(A)$
for ($j \in (1, \dots, r)$):
 $x_j \leftarrow Replace(x_j)$
end for
 Replace r segments into S to generate S'
return S'

2) *Attack Setup*: The attacker aims to create adversarial patches capable of effectively deceiving the victim deep learning-based classifier. We generate distinct patches in five different sizes: 38×38 , 41×41 , 44×44 , 47×47 , and 50×50 . In the case of the LaVAN patch, the patch's location is fixed to the upper left corner of the image. Conversely, for GoogleAp, the patch is randomly placed within the image (refer to Figure 3). Each patch undergoes a training process consisting of 100 epochs, utilizing a training dataset comprising 1000 images. Subsequently, we evaluate the attack success rate on a separate test dataset. In the context of ImageNet, our evaluation encompasses a set of 10,000 images sampled from the validation dataset.

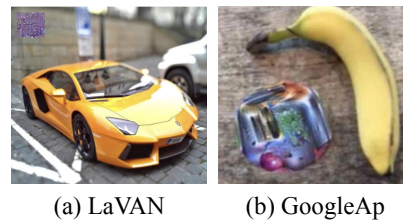


Fig. 3: Patch based attacks: a) LaVAN [18], b) GoogleAp [19].

3) *Defense Setup*: The defense mechanism comprises of three phases, as described in Section III. For the Segmenting Phase, we varied the kernel size from 40×40 pixels to 20×20 pixels and a stride length 5 to 10 pixels and the most optimal performance with respect to downstream accuracy on the task was observed for kernel size 40×40 and stride length 8 pixels. For the Isolating Phase, for the DBSCAN algorithm, we tuned

the hyper-parameters with respect to downstream accuracy and used $\text{eps} = 0.4$ and $\text{minPts} = 1201$.

B. Experimental Results

In our evaluation, we primarily focused on quantifying the model’s robust accuracy. To demonstrate the efficacy of our defense strategy, we initially generated adversarial patches using two distinct attack methodologies: LAVAN and GoogleAp. Subsequently, we assessed the model’s robust accuracy across various patch sizes and different models. The baseline performances of our defense on clean samples without patches were measured as follows: 81.2% (ResNet-152), 78.4% (ResNet-50), and 74.2% (VGG-19) on the ImageNet dataset, and 94.1% (ResNet-152), 90.9% (ResNet-50), and 88.6% (VGG-19) on the CalTech-101 dataset.

Tables I and II demonstrate the notable effectiveness of our defense technique, illustrating a remarkable level of robust accuracy in mitigating GoogleAp and LAVAN attacks on the ImageNet dataset. For instance, our defense achieves robust accuracy rates of 67.1% and 63.6% when employed against GoogleAp and LAVAN attacks, respectively, for the ResNet-50 model and a patch size 38×38 .

TABLE I: Robustness on GoogleAp attack (ImageNet dataset)

Patch Size	Model / Neural Network	Baseline Accuracy	Adversarial Accuracy	Robustness (w/ patch)
38	ResNet 152	81.2%	39.9%	64.8%
x	ResNet 50	78.4%	38.8%	67.1%
38	VGG 19	74.2%	39.1%	63.7%
41	ResNet 152	81.2%	21.4%	67.1%
x	ResNet 50	78.4%	21.1%	67.2%
41	VGG 19	74.2%	22.8%	61.4%
44	ResNet 152	81.2%	14.6%	70.8%
x	ResNet 50	78.4%	14.2%	60.9%
44	VGG 19	74.2%	15.8%	63.9%
47	ResNet 152	81.2%	9.3%	69.4%
x	ResNet 50	78.4%	9.0%	64.7%
47	VGG 19	74.2%	10.6%	60.3%
50	ResNet 152	81.2%	4.9%	65.8%
x	ResNet 50	78.4%	4.5%	67.4%
50	VGG 19	74.2%	3.8%	63.1%

Similarly, on the Caltech-101 dataset (refer to Tables III and IV), our defense exhibits outstanding performance, achieving robust accuracy rates of 76.5% and 73.6% when countering GoogleAp and LAVAN attacks, respectively, for the ResNet-50 model with a patch size of 38×38 .

C. Comparison with SOTA

We conduct a comparative analysis of our defense mechanism against LGS [1] and Jujutsu [2]. Additionally, for comparative purposes, we compare our technique with two certified defenses—namely, De-randomized smoothing (DS) [15] and PatchGuard [14].

As demonstrated in Table V, our defense strategy outperforms state-of-the-art techniques. Specifically, our approach

TABLE II: Robustness on LAVAN attack (ImageNet dataset)

Patch Size	Model / Neural Network	Baseline Accuracy	Adversarial Accuracy	Robustness (w/ patch)
38	ResNet 152	81.2%	10.1%	63.1%
x	ResNet 50	78.4%	10.2%	63.6%
38	VGG 19	74.2%	11.1%	60.5%
41	ResNet 152	81.2%	7.9%	68.2%
x	ResNet 50	78.4%	8.3%	61.8%
41	VGG 19	74.2%	8.1%	57.1%
44	ResNet 152	81.2%	4.9%	66.1%
x	ResNet 50	78.4%	4.8%	64.7%
44	VGG 19	74.2%	4.8%	61.8%
47	ResNet 152	81.2%	1.2%	65.8%
x	ResNet 50	78.4%	1.0%	68.9%
47	VGG 19	74.2%	1.7%	58.6%
50	ResNet 152	81.2%	1.9%	63.2%
x	ResNet 50	78.4%	2.0%	62.1%
50	VGG 19	74.2%	2.1%	61.5%

TABLE III: Robustness on GoogleAp attack (CalTech-101)

Patch Size	Model / Neural Network	Baseline Accuracy	Adversarial Accuracy	Robustness (w/ patch)
38	ResNet 152	94.1%	48.6%	81.7%
x	ResNet 50	90.9%	49.2%	76.5%
38	VGG 19	88.6%	47.1%	71.9%
41	ResNet 152	94.1%	30.1%	78.8%
x	ResNet 50	90.9%	29.3%	74.1%
41	VGG 19	88.6%	28.2%	75.9%
44	ResNet 152	94.1%	10.8%	80.5%
x	ResNet 50	90.9%	11.2%	75.3%
44	VGG 19	88.6%	12.6%	75.1%
47	ResNet 152	94.1%	9.1%	77.4%
x	ResNet 50	90.9%	9.6%	75.4%
47	VGG 19	88.6%	10.4%	73.1%
50	ResNet 152	94.1%	6.8%	77.4%
x	ResNet 50	90.9%	5.9%	76.1%
50	VGG 19	88.6%	6.2%	71.3%

achieves a robust accuracy of 67.1%, surpassing LGS, Jujutsu, and Jedi defenses, which achieve robust accuracy rates of 53.86%, 60%, and 64.34%, respectively.

D. Key Findings

The key conclusions from the experimental observations are mentioned here:

- The proposed defense technique against adversarial patch attacks is successful in providing robustness to the image classification task, with up to 28% recovery for the standard 38×38 pixel patch size.
- The performance is consistent across different patch sizes, for various neural architectures and datasets.

TABLE IV: Robustness on LAVAN attack (CalTech-101)

Patch Size	Model / Neural Network	Baseline Accuracy	Adversarial Accuracy	Robustness (w/ patch)
38	ResNet 152	94.1%	15.6%	77.2%
x	ResNet 50	90.9%	17.1%	73.6%
38	VGG 19	88.6%	15.3%	73.1%
41	ResNet 152	94.1%	14.2%	79.2%
x	ResNet 50	90.9%	13.9%	74.2%
41	VGG 19	88.6%	13.8%	72.2%
44	ResNet 152	94.1%	8.4%	76.8%
x	ResNet 50	90.9%	8.9%	77.7%
44	VGG 19	88.6%	9.1%	71.2%
47	ResNet 152	94.1%	5.1%	76.8%
x	ResNet 50	90.9%	4.9%	73.4%
47	VGG 19	88.6%	6.1%	73.8%
50	ResNet 152	94.1%	1.2%	77.5%
x	ResNet 50	90.9%	1.0%	74.8%
50	VGG 19	88.6%	1.8%	73.9%

TABLE V: Performance of our proposed defense compared to four state-of-the-art defenses against GoogleAp [19] attack.

Defense	Robust Accuracy
LGS [1]	53.86%
DS [15]	35.02%
PatchGuard [14]	30.96%
Jujutsu [2]	60%
Ours	67.1%

- It is also able to outperform the state-of-the-art with 67.1% robust accuracy for ResNet-50 on the ImageNet dataset.

V. POTENTIAL ADAPTIVE ATTACK

In order to generate a patch capable of circumventing our defense, the adversarial noise must adhere to a distribution similar/close to that of clean images. We implement the adaptive attack by constraining the distribution of the adversarial patch to closely match the average distribution of n randomly selected fragments from the clean image. Specifically, we calculate the average distribution in terms of both mean and standard deviation. We then compute the mean difference and standard deviation ratio between the average distribution of the fragments and the adversarial patch.

We compute the mean and standard deviation separately for each channel of the patch, and adjust the gradient of each channel accordingly. This ensures that the mean and standard deviation constraints are enforced for each channel of the adversarial patch during optimization. $0.02 \leq |\mu - m| \leq 0.08$ $1.5 \leq \sigma/std \leq 2.4$ We recalculated the Mahalanobis distance for each segment and plotted them. Upon observation, we noticed a one single heavy tailed distribution indicating that the segments located on the adversarial patch exhibited a Mahalanobis distance closer to that of the rest of the image

segments (See Figure 4) which makes it challenging to isolate the patch as anomalies. In addition, the generated patch was only able to decrease model accuracy from 78% to 67% for ResNet50 on ImageNet, demonstrating that it is difficult to generate an adversarial patch that will not behave as an anomaly as compared to the distribution of the image.

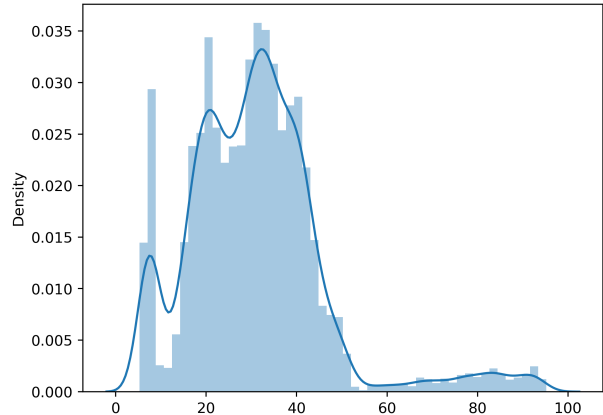


Fig. 4: Plot of Mahalanobis distances of segments upon introducing the adaptive attack, showing one single heavy tailed distribution.

VI. RELATED WORKS

Defenses against adversarial patch-based attacks can be broadly classified into two categories: certified defenses and empirical defenses.

Certified defenses: **De-randomized Smoothing (DS)** [15] introduces a certified defense technique by building a smoothed classifier through ensembling local predictions made on pixel patches. **PatchGuard** [14] employs a small receptive field within deep neural networks (DNNs) and secures feature aggregation by masking out regions with the highest sum of class evidence.

Empirical defenses: **Localized Gradient Smoothing (LGS)** [1] normalizes gradient values and utilizes a moving window to identify high-density regions based on specific thresholds. **Jujutsu** [2] focuses on localizing adversarial patches and distinguishing them from benign samples.

While these defenses offer valuable contributions, they are not without limitations, including high false positive rates and poor detection rates. Additionally, a significant challenge lies in effectively mitigating the adversarial impact while ensuring deep neural networks (DNNs) make accurate inferences on clean examples.

VII. CONCLUSION

Adversarial patch based attacks are a common and practical mode of exposing vulnerabilities in trained neural networks to behave erroneously for image classification tasks. In this paper, we have proposed a defense mechanism that makes

use of the insight that the said adversarial patches contain information or variability which is significantly different from the data distribution in the rest of the image. This helps us in using clustering based anomaly detection techniques to isolate the patches. We have proposed a three-step pipeline for the same and have reported impressive performance. In the future, the objective is to make this technique more robust by developing stronger anomaly detection techniques and extending the defense mechanism to other computer vision tasks.

REFERENCES

- [1] M. Naseer, S. Khan, and F. Porikli, "Local gradients smoothing: Defense against localized adversarial attacks," in *2019 IEEE Winter Conference on Applications of Computer Vision (WACV)*. IEEE, 2019, pp. 1300–1307.
- [2] Z. Chen, P. Dash, and K. Pattabiraman, "Jujutsu: A two-stage defense against adversarial patch attacks on deep neural networks," in *Proceedings of the 2023 ACM Asia Conference on Computer and Communications Security*, ser. ASIA CCS '23. New York, NY, USA: Association for Computing Machinery, 2023, p. 689–703.
- [3] A. Guesmi, M. A. Hanif, B. Ouni, and M. Shafique, "Physical adversarial attacks for camera-based smart systems: Current trends, categorization, applications, research challenges, and future outlook," *IEEE Access*, 2023.
- [4] N. Carlini and D. A. Wagner, "Towards evaluating the robustness of neural networks," *CoRR*, vol. abs/1608.04644, 2016. [Online]. Available: <http://arxiv.org/abs/1608.04644>
- [5] B. Li and Y. Vorobeychik, "Scalable optimization of randomized operational decisions in adversarial classification settings," in *Proceedings of the Eighteenth International Conference on Artificial Intelligence and Statistics, AISTATS 2015, San Diego, California, USA, May 9-12, 2015*, ser. JMLR Workshop and Conference Proceedings, G. Lebanon and S. V. N. Vishwanathan, Eds., vol. 38. JMLR.org, 2015. [Online]. Available: <http://proceedings.mlr.press/v38/li15a.html>
- [6] I. J. Goodfellow, J. Shlens, and C. Szegedy, "Explaining and harnessing adversarial examples," *CoRR*, vol. abs/1412.6572, 2015.
- [7] N. Chattopadhyay, A. Chattopadhyay, S. S. Gupta, and M. Kasper, "Curse of dimensionality in adversarial examples," in *2019 International Joint Conference on Neural Networks (IJCNN)*. IEEE, 2019, pp. 1–8.
- [8] N. Chattopadhyay, S. Chatterjee, and A. Chattopadhyay, "Robustness against adversarial attacks using dimensionality," in *International Conference on Security, Privacy, and Applied Cryptography Engineering*. Springer, 2021, pp. 226–241.
- [9] A. Guesmi, R. Ding, M. A. Hanif, I. Alouani, and M. Shafique, "Dap: A dynamic adversarial patch for evading person detectors," 2023.
- [10] A. Guesmi, I. M. Bilasco, M. Shafique, and I. Alouani, "Advart: Adversarial art for camouflaged object detection attacks," *arXiv preprint arXiv:2303.01734*, 2023.
- [11] Y.-C.-T. Hu, J.-C. Chen, B.-H. Kung, K.-L. Hua, and D. S. Tan, "Naturalistic physical adversarial patch for object detectors," in *2021 IEEE/CVF International Conference on Computer Vision (ICCV)*, 2021, pp. 7828–7837.
- [12] A. Guesmi, M. A. Hanif, B. Ouni, and M. Shafique, "Saam: Stealthy adversarial attack on monocular depth estimation," *IEEE Access*, 2024.
- [13] A. Guesmi, M. A. Hanif, I. Alouani, and M. Shafique, "Aparate: Adaptive adversarial patch for cnn-based monocular depth estimation for autonomous navigation," *arXiv preprint arXiv:2303.01351*, 2023.
- [14] C. Xiang, A. N. Bhagoji, V. Sehwal, and P. Mittal, "{PatchGuard}: A provably robust defense against adversarial patches via small receptive fields and masking," in *30th USENIX Security Symposium (USENIX Security 21)*, 2021, pp. 2237–2254.
- [15] A. Levine and S. Feizi, "(de) randomized smoothing for certifiable defense against patch attacks," *Advances in Neural Information Processing Systems*, vol. 33, pp. 6465–6475, 2020.
- [16] M. Ester, H.-P. Kriegel, J. Sander, X. Xu *et al.*, "A density-based algorithm for discovering clusters in large spatial databases with noise," in *kdd*, vol. 96, no. 34, 1996, pp. 226–231.
- [17] E. Schubert, J. Sander, M. Ester, H. P. Kriegel, and X. Xu, "Dbscan revisited, revisited: why and how you should (still) use dbscan," *ACM Transactions on Database Systems (TODS)*, vol. 42, no. 3, pp. 1–21, 2017.
- [18] D. K. et al., "Lavan: Localized and visible adversarial noise," in *International Conference on Machine Learning*, 2018.
- [19] T. B. et al., "Adversarial patch," 2017. [Online]. Available: <https://arxiv.org/pdf/1712.09665.pdf>
- [20] A. Athalye, L. Engstrom, A. Ilyas, and K. Kwok, "Synthesizing robust adversarial examples," in *International conference on machine learning*. PMLR, 2018, pp. 284–293.
- [21] K. I. Penny, "Appropriate critical values when testing for a single multivariate outlier by using the mahalanobis distance," *Journal of the Royal Statistical Society: Series C (Applied Statistics)*, vol. 45, no. 1, pp. 73–81, 1996.
- [22] R. De Maesschalck, D. Jouan-Rimbaud, and D. L. Massart, "The mahalanobis distance," *Chemometrics and intelligent laboratory systems*, vol. 50, no. 1, pp. 1–18, 2000.
- [23] G. J. McLachlan, "Mahalanobis distance," *Resonance*, vol. 4, no. 6, pp. 20–26, 1999.
- [24] D. Birant and A. Kut, "St-dbscan: An algorithm for clustering spatial-temporal data," *Data & knowledge engineering*, vol. 60, no. 1, pp. 208–221, 2007.
- [25] A. Smiti and Z. Elouedi, "Dbscan-gm: An improved clustering method based on gaussian means and dbscan techniques," in *2012 IEEE 16th international conference on intelligent engineering systems (INES)*. IEEE, 2012, pp. 573–578.
- [26] J. Deng, W. Dong, R. Socher, L.-J. Li, K. Li, and L. Fei-Fei, "Imagenet: A large-scale hierarchical image database," in *2009 IEEE Conference on Computer Vision and Pattern Recognition*, 2009, pp. 248–255.
- [27] K. He, X. Zhang, S. Ren, and J. Sun, "Deep residual learning for image recognition," 2015.
- [28] K. Simonyan and A. Zisserman, "Very deep convolutional networks for large-scale image recognition," 2015.